RESEARCH PAPER

The behavior of TIG welding arc in a high-frequency axial magnetic field

H. Wu [1,2] · Y. L. Chang [1] · Alexandr Babkin [3] · Boyoung Lee [4]

Abstract

The effect of high-frequency axial magnetic field (HFAMF) on the shape of the welding arc and welding formation of tungsten inert gas (TIG) welding is analyzed theoretically and experimentally. The 316L stainless steel plate was welded with HFAMF produced by the excitation coil installed on the welding torch. The influence of the HFAMF on the welding process is studied by changing the magnetic frequency from 0 to 2000 Hz. The experimental results show that when the magnetic field frequency reaches 1500 Hz, the arc rotation radius is decreased to the minimum; the arc shape changes from cone to compressed cylinder; and the arc temperature, the arc pressure, and the depth-width ratio of the weld beam reached the maximum. Otherwise, the effect of applied HFAMF on the stress of arc and weld pool is discussed, and the mechanism of arc contraction is analyzed.

Keywords High-frequency magnetic field · Magnetic confinement · Arc plasma · TIG

1 Introduction

The tungsten inert gas (TIG) welding method has been applied frequently owing to its advantages, such as better shielding, stable arc, easy adjustment of heat input, less material splash, easy to monitor the weld pool and arc conditions, and neat welding appearance. However, the lower deposition rates and low production efficiency limit its application. To make this process more suitable for the fabrication of large structures and thick weldments, the magnetic field is applied around the arc to improve production efficiency.

The external magnetic fields can alter the arc plasma effectively. Previous research has shown that different types of magnetic fields will have different effects on the arc shape, the distribution of energy density, and the weld appearance [1]. As an example, Chang et al. [2] found that the axial magnetic field can rotate the CO_2 arc and change its radius; Nomura et al. [3] considered that the cusp magnetic field makes the arc cross section elliptical and the depth-width ratio of the weld increase. Li et al. [4] found that the external longitudinal magnetic field could offset the arc along the weld direction, to effectively prevent the appearance of a hump in high-speed welding. Sun et al. [5] found that the transverse magnetic field causes the arc to oscillate perpendicular to the direction of the weld, which can effectively prevent insufficient sidewall fusion and improve efficiency and quality of thick component welding during narrow gap welding. Wang et al. [6] found that the rotating magnetic field causes the arc to rotate and the arc axis to deviate from the original axis. Yin et al. [7–15] established a 3D numerical model containing the welding arc and the cathode or welding arc and the weld pool for TIG with applied DC or low-frequency axial magnetic field. Based on the theoretical calculation and numerical simulation of the temperature field, velocity field, pressure field, and current density of plasma arc and weld pool, all the

✉ Y. L. Chang
495930535@qq.com

H. Wu
hebeuwh@126.com

Alexandr Babkin
bas43@yandex.ru

Boyoung Lee
bylee@kau.ac.kr

[1] Shenyang University of Technology, No. 111, Shenliao West Road, Economic & Technological Development Zone, Shenyang 110870, People's Republic of China

[2] Hebei University of Engineering, Handan 056038, China

[3] Lipetsk State Technical University, 398024 Lipetsk, Russia

[4] Korea Aerospace University, Seoul 412791, South Korea

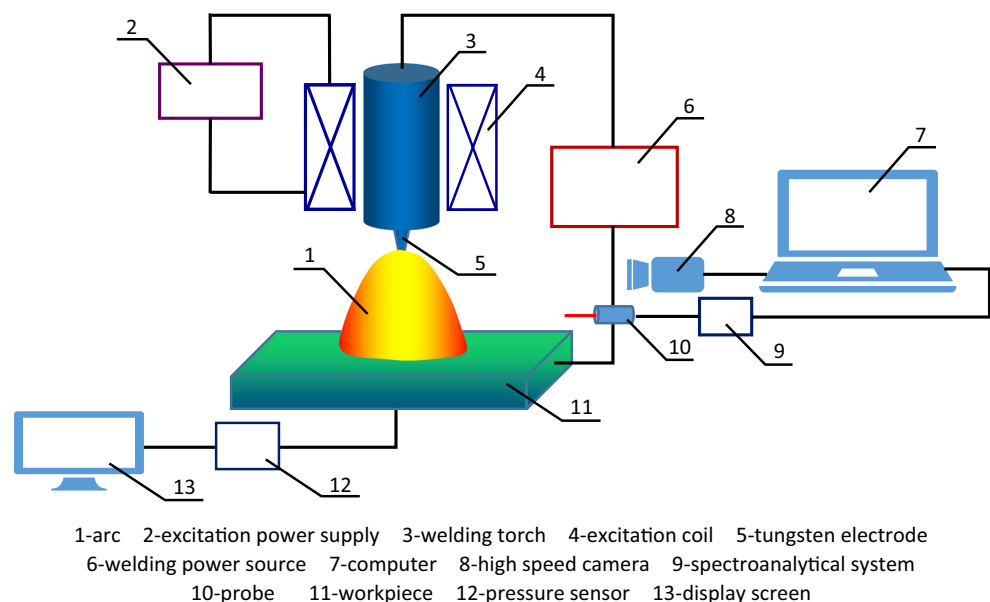**Table 1** Chemical composition of stainless steel strip (wt%)

C	Si	Mn	Ni	Cr	Mo	S	P
0.030	≤ 1.000	≤ 2.000	10.00~14.00	16.00~18.00	2.00~3.00	≤ 0.030	≤ 0.045

driving forces that influence the fluid flow of the weld arc and pool are analyzed to explain these phenomena, such as the distribution of temperature, heat flux density, current density, and arc pressure on the anode surface presents bimodal carve, as well as the formation of wide and shallow weld pool. The mechanism of the shape of TIG arc and pool changes with the applied axial magnetic field is clarified. Their researches provide a solid foundation for further understanding the physical nature of welding arc and pool. This article focuses on the influence of the high-frequency axial magnetic field on the TIG arc, to explore the mechanism of the external magnetic field on the arc plasma, comprehensively and systematically.

2 Experimental method

The base metal is 316 L (00Cr17Ni14Mo2) and the thickness of the stainless steel strip is 3 mm; the compositions of the stainless steel band are shown in Table 1. A high-frequency axial alternating magnetic field is added to the TIG welding arc by a high-frequency excitation device; the experimental device is shown in Fig. 1 and comprises a high-speed video camera to acquire the TIG welding arc image; a spectroanalytical system composed of AvaSpec-USB2.0 multi-channel high-resolution instant spectrometer to measure the arc temperature and the pressure sensors model DTR-131 is connected to the CYG1103 pressure transmitter to measure

the arc pressure and its distribution. The high-frequency axial magnetic field is generated by the magnetic head installed on the welding torch, and the structure of the magnetic head is shown in Fig. 2.

The welding parameters of TIG welding process are shown in Table 2. To study the influence of the frequency of the additional magnetic field on the welding arc, a magnetic field generator that can produce high- and low-frequency axial magnetic fields has been developed, and the frequency of the external magnetic fields is shown in Table 3.

In the experiment, the duty ratio of the alternating axial magnetic field is 50%.

3 Results and discussion

3.1 The arc shape

The results of the experiment are summarized in Fig. 3. In this experiment, the magnetic induction intensity at 1 mm below the solenoid is measured by a Corey G201 type Tesla meter and the testing value is 30 mT. The welding arc shape is captured by a high-speed video camera. The results show that the welding arc rotates under the action of the external axial magnetic field, and the higher the frequency of the magnetic field, the faster the rotational speed of the arc.

Fig. 1 Illustration of experimental device

1-arc   2-excitation power supply   3-welding torch   4-excitation coil   5-tungsten electrode
6-welding power source   7-computer   8-high speed camera   9-spectroanalytical system
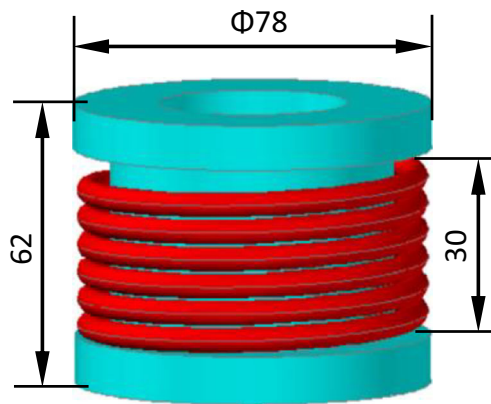10-probe   11-workpiece   12-pressure sensor   13-display screen

Fig. 2 Structure of the magnetic head

By comparing multiple sets of high-speed photographs, it can be found that the shape of the welding arc is changed after the additional axial magnetic field is applied to the TIG welding. When the frequency is low, the bottom of the arc expands, the top of the arc arch rises, and the shape of the arc changes from the original conical shape of the arc with no applied field to a bell-shaped cover. When the frequency reaches 120 Hz, the arc becomes very unstable. When the frequency reaches 500 Hz, the arc tends to stabilize. When the frequency reaches 1000 Hz, the arc is stable and contracts radially. When the frequency of the additional magnetic field reaches 1500 Hz, the cross section of the arc shrinks to a minimum and the arc shape changes from the bell shape into an approximate cylinder shape. When the frequency continues to increase, the arc re-diverges.

Comparing the two illustrations in Fig. 3, the effect of the magnetic field frequency on the arc shape shows the same trends. With the frequency of the magnetic field increased, the arc plasma is first distributed to the bell shape and then to the cylinder; it then re-diverges, regardless of whether the welding current is 70 A or 100 A. The best compression effect of the arc is seen when the frequency of the magnetic field is 1500 Hz.

To analyze the variation in regularity of the arc shape with an increase in the magnetic field frequency, the conical angle of arc is measured and compared, as shown in Fig. 4. It can be seen clearly from the figure that when the magnetic field frequency is less than 500 Hz, the conical angle of arc first increases and then decreases, next fluctuates within a certain range with the increase of magnetic field frequency; however,

the conical angle of magnetic-control arc is always greater than that of the arc with no applied field. When the frequency of the magnetic field is higher than 500 Hz, the conical angle of arc first decreases and then increases, and it is always smaller than that of the arc with no applied field. The conical angle of arc is the smallest when the frequency of magnetic field is 1500 Hz.

3.2 The arc pressure

The arc pressure is measured by the pressure sensor, and the curve of the arc pressure distribution is drawn, when the welding current is 70 A. The distribution of arc plasma pressure changes from annular bimodal for low-frequency magnetic field to single peak for high-frequency magnetic field. The peak also is higher than the conventional single peak without a magnetic field, as shown in Fig. 5. The results show that with an increase in magnetic field frequency, the arc center pressure decreases quickly. When the frequency is raised to 50 Hz, the arc center pressure is negative. However, when the frequency is further increased to 500 Hz, the annular bimodal suddenly disappears and becomes a single peak. It can also be observed that with an increase in the frequency, the center pressure of the arc plasma also increases and reaches maximum for a frequency of 1500 Hz. Meanwhile, the diameter of the crest circle of the annular bimodal first increases and then decreases until it disappears, as shown in Fig. 5. When the welding current is 100 A, the arc pressure distribution is the same as when it is 70 A.

3.3 The arc temperature

The temperature of the arc center at 1 mm below tungsten is measured by optical emission spectroscopy and calculated by Boltzmann diagram method; the effects of the frequency of the magnetic fields on the temperature of the arc center are compared, and the curve of the temperature of the arc center is drawn in Fig. 6. It shows that with an increase in magnetic field frequency, the temperature of the arc center decreases at first, then rises to a maximum value, then decreases, and finally maintains a trend with minimal amplitude fluctuation. At low frequency (≤ 300 Hz), the temperature of the arc center is always lower than the temperature of the arc center without the applied magnetic field, but at high frequency (> 500 Hz), the temperature of the arc center is higher than that of the arc

Table 2 Welding experiment parameters

Group	Welding current/A	Arc length/ mm	Tungsten electrode diameter/mm	Shielding gas flow rate/min	Excitation current/A	Excitation coil turns	Shutter speed/s	The duty ratio
I	70	3	2.4	12	20	6	1/2000	50%
II	100	3	2.4	12	20	6	1/2000	50%

Table 3 Magnetic field frequency parameters

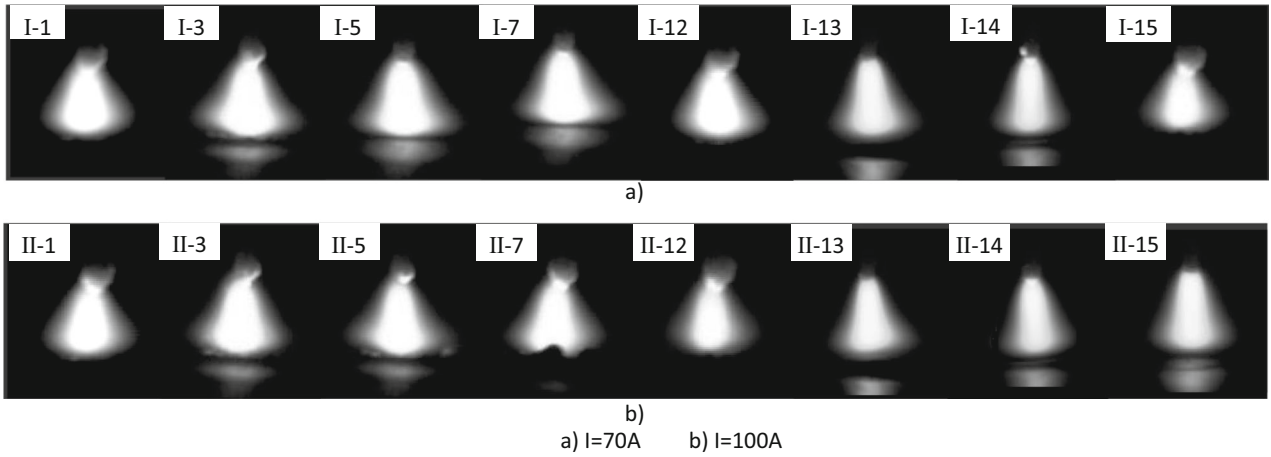| Sample	1	2	3	4	5	6	7	8	9	10	11	12	13	14	15	16
Frequency/Hz	0	5	10	20	50	80	120	200	300	500	800	1000	1200	1500	1800	2000

a) I=70A   b) I=100A

Fig. 3 Arc shape with different parameters

center without the applied field. When the welding current is 70 A and the magnetic induction intensity is about 30 mT and the magnetic frequency is 1500 Hz, the center temperature of the arc is highest, and it has increased by about 730 K compared with that of the arc with no applied field, while the maximum difference in temperature between the compressed arc and the arc with no applied field is about 550 K when the welding current is 100 A. It can be seen from the Figs. 3 and 5 that when the excitation frequency is 1500 Hz, the compression effect of the external axial magnetic field on the arc is the best, and the values of the temperature rise of the arc are the largest. Moreover, the effect of arc contraction and arc

temperature rise is more evident when the welding current is 70 A than when the current is 100 A.

3.4 The weld appearance

The appearance of TIG welding with additional axial magnetic field is compared in Fig. 7 when the welding current is 70 A. It can be seen from the figure that the change of magnetic field frequency will lead to the changes of weld width and penetration. Combined with Figs. 4 and 6, it is obvious
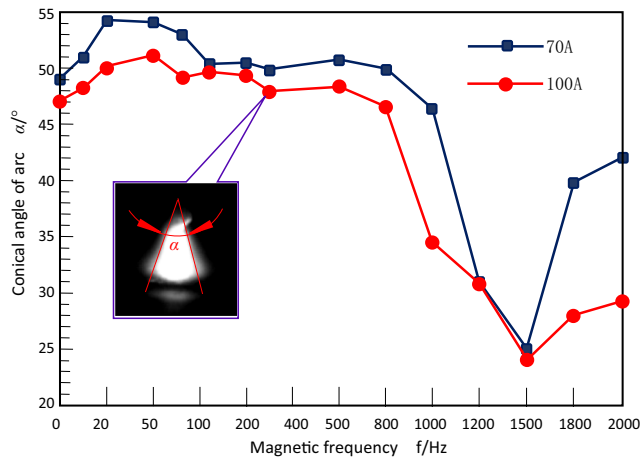

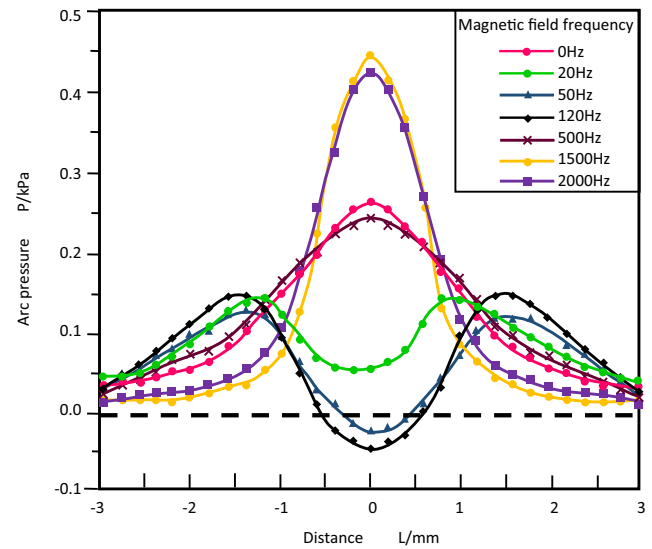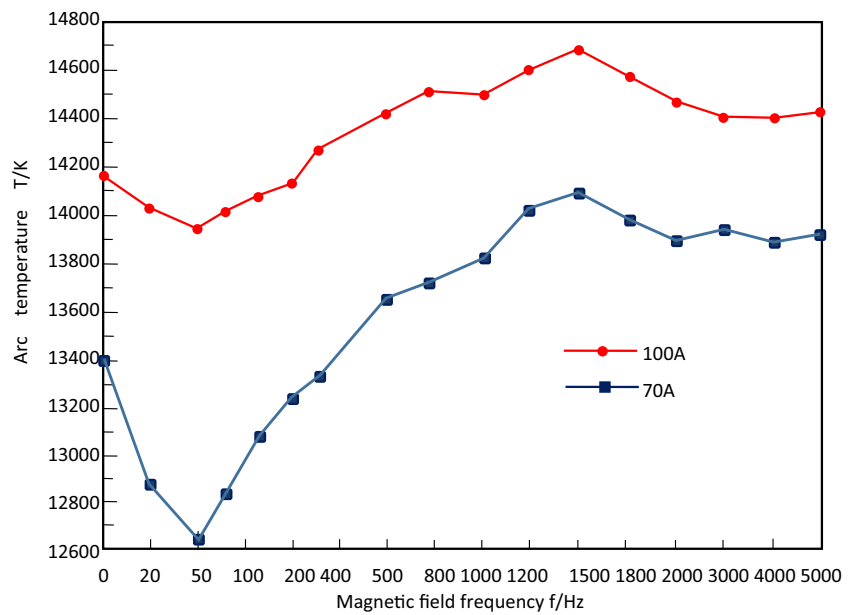**Fig. 4** The relationship of magnetic frequency and conical angle of arc

**Fig. 5** The distribution of arc pressure

Fig. 6 Arc temperatures with magnetic field frequencies

that with the increase of conical angle of arc, the arc temperature decreases, the width of TIG weld increases, and the penetration decreases. When the frequency of magnetic field is less than 500 Hz, with an increase in the magnetic field frequency, the weld width first increases and then decreases, and the weld penetration first decreases and then increases.

When the magnetic field frequency is greater than 500 Hz, the weld width decreases and the penetration increases with the increase of magnetic field frequency. When the magnetic field frequency reaches 1500 Hz, the weld penetration is the largest and the weld width is the smallest. Compared with the weld forming without magnetic field, the penetration depth

Fig. 7 Influence of magnetic field frequency on weld seam cross section profile
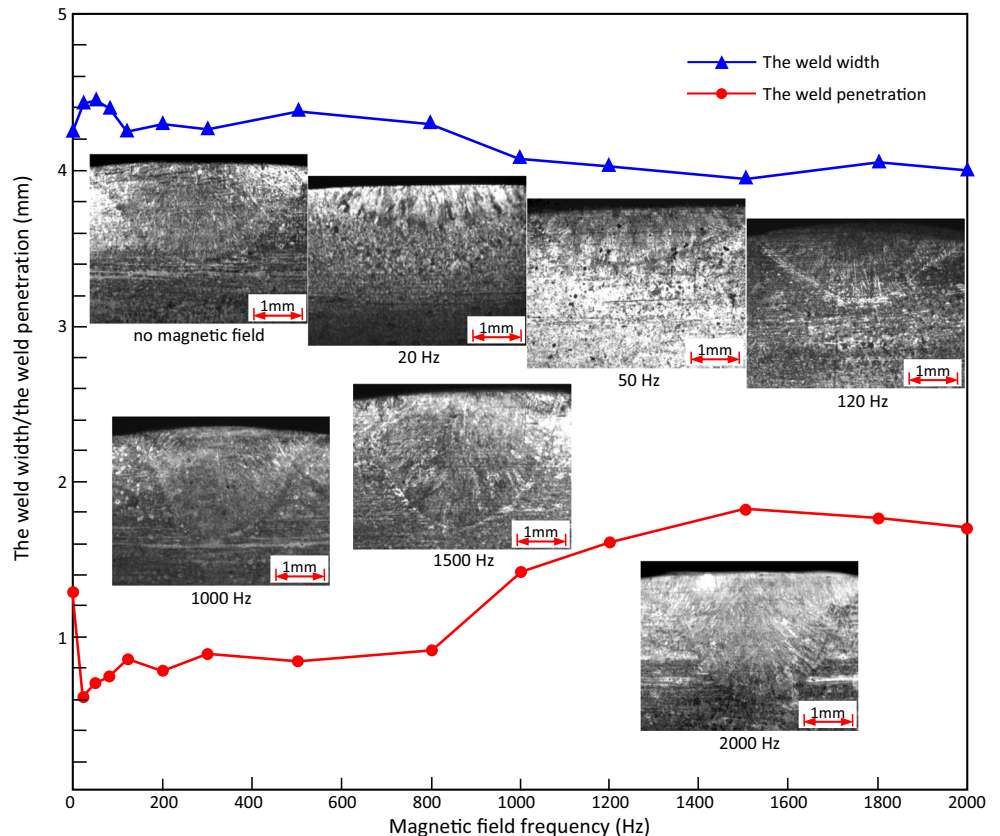
increases from 1.28 to 1.83 mm, an increase of about 43%, and the weld width decreases from 4.24to 3.90 mm, a decrease of 8%.

3.5 Mechanism analysis of arc compression

Because the density and temperature of the plasma arc are larger in the upper portion than in the lower portion of the arc, the shape of the arc with no applied field is conical. The diamagnetic effect of the arc plasma will repel the magnetic field added to its boundary and the welding arc itself is not a homogeneous conductor; the resistance of the arc at the center is small but the temperature is high, and the resistance at the arc edge is high but the temperature is low. In addition, the flux density of the solenoid magnetic field passing through the core is higher owing to the existence of the annular core, so the distribution of the external magnetic field is not uniform; the magnetic field lines are concentrated at the edge of arc but scattered in the center of the arc, as shown in Fig. 8.

The external axial magnetic field creates a Lorentz force, which makes the arc plasma rotate and spiral down to the anode [7]. The rotating arc induces a "magneto-hydro dynamics (MHD) pumping effect", which significantly enhances axial flow in front of the cathode tip, so that the arc near the cathode tip is compressed and a higher temperature is produced [8]. At the same time, the centrifugal flow generated by the plasma rotation arises an accumulation ring on the anode surface, where the pressure is the highest. The plasma is forced to flow to the center and forming a reverse vortex. The reverse vortex makes the plasma flow from anode to cathode along the central axis, and then flows outward and downward, as shown in Fig. 9 [7], and produces a larger low temperature hollow and negative pressure zone near the anode
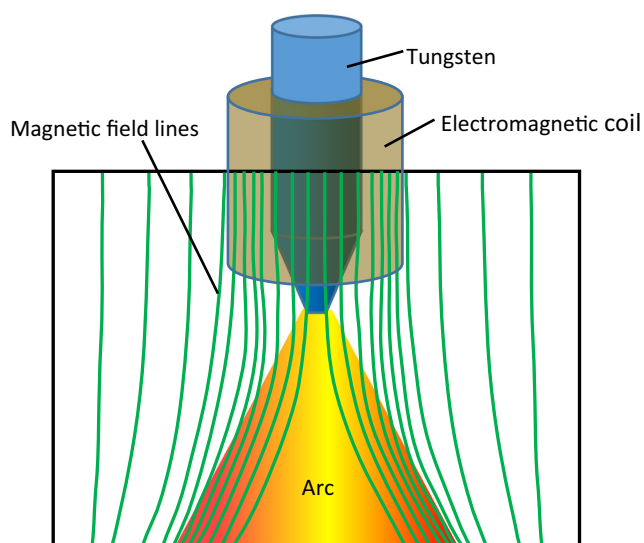

Fig. 8 The effect of arc plasma on distribution of magnetic field lines
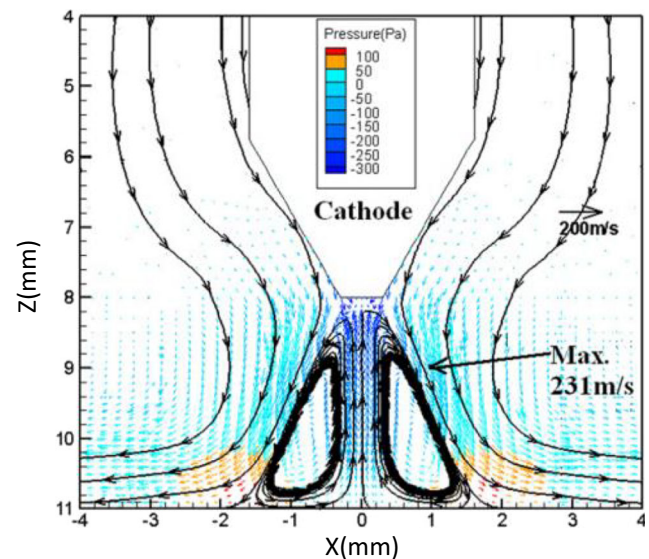

Fig. 9 Velocity of the arc plasma on the axial section ($B = 0.02$ T) [7]

[8–11]. The low temperature cavity promotes the metal vapor to generate like a "fountain" [12].

Under the action of Lorentz force, the trajectory of charged particles is spiral, as shown in Fig. 10. Due to the great difference in the mass of electron and argon ion, the radius and the period of gyration are quite different when the axial magnetic field is applied. Take an argon ion in the upper part of the arc as the research object, and its trajectory is shown in the solid line in Fig. 10a. The dotted lines show the trajectories of argon ions at other positions. Obviously, the motion of argon ion causes the arc plasma to rotate around its axis under the action of axial magnetic field. The trajectory of the electron is different from that of argon ion. It will spiral around the magnetic field line, as shown in Fig. 10b. The centrifugal force generated by the rotation and the confinement effect on electrons by nonuniform magnetic field make the charged particles gather below the cathode and the edge of arc and produce a larger low-temperature hollow and negative pressure area above anode, as shown in Fig. 11. Ignoring aerodynamic resistance and gravity, the forces acting on charged particles include Lorentz force F_B generated by external magnetic field, electric force F_E, viscous force F_V, and pressure F_P, which is the pressure difference between the inside and outside of the arc caused by the negative pressure and the hollow. The forces on argon-ion are shown in Fig. 11, the red ball represents the argon ion on the outer surface of the arc, and the blue ball represents the argon ion inside the arc. It can be seen that the Lorentz force F_B and pressure F_P make the argon ions on the outer surface of the arc move towards the arc center, while the "fountain" effect of metal vapor makes the argon ions at the edge of the hollow above the anode move to the outside of the arc under the pressure F_P. Therefore, the general trend is that the particles in the upper part move from the arc edge to the arc center, while the particles in the lower part move from the arc center

Fig. 10 The trajectory of argon-ion and electron in the arc. **a** The trajectory of argon-ion. **b** The trajectory of electron. (i) Positive half cycle. (ii) Negative half cycle

i) positive half cycle   ii) negative half cycle

a) the trajectory of argon-ion   b) the trajectory of electron
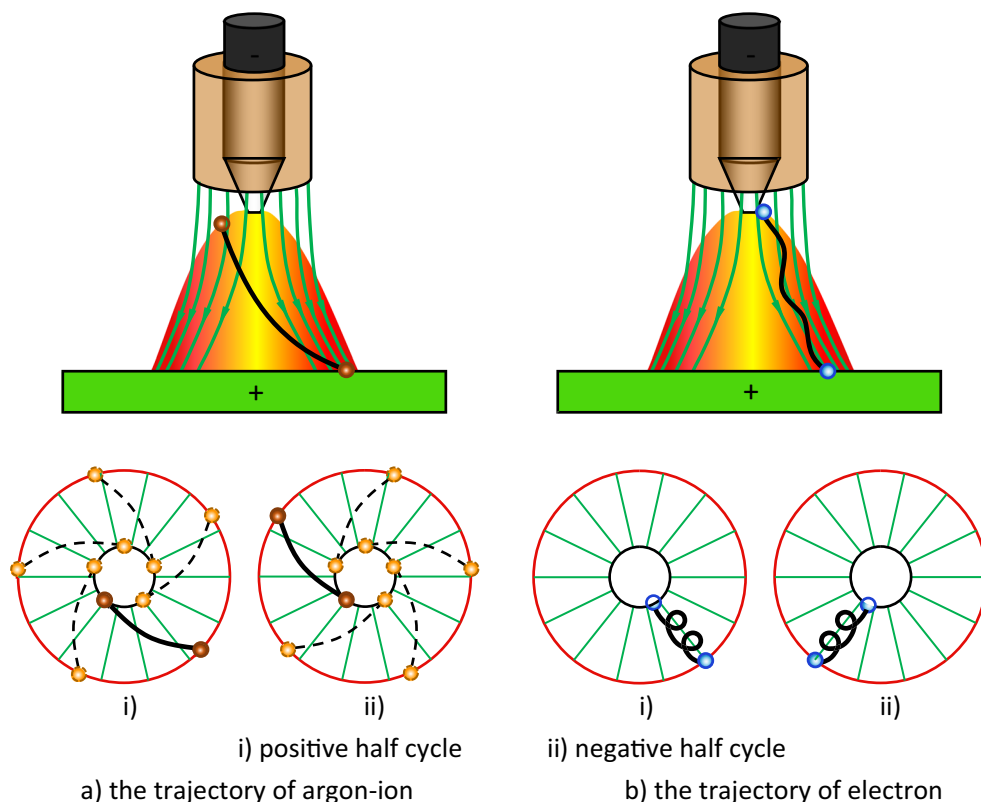
to the arc edge, so the arc shrinks at the top and expands at the bottom [13].

If an alternating axial magnetic field is applied, when the direction of the magnetic field changes, the charged particles rotate in reverse, as shown in Fig. 10 (ii). The change of the

magnetic field direction slows the plasma rotation above the anode surface, and the centrifugal force is also significantly reduced. Therefore, the charged particles gather under the tungsten electrode, causing the luminous region of the arc to elongate, the central negative pressure area to decrease or even

Fig. 11 The forces on argon-ion under external axial magnetic field

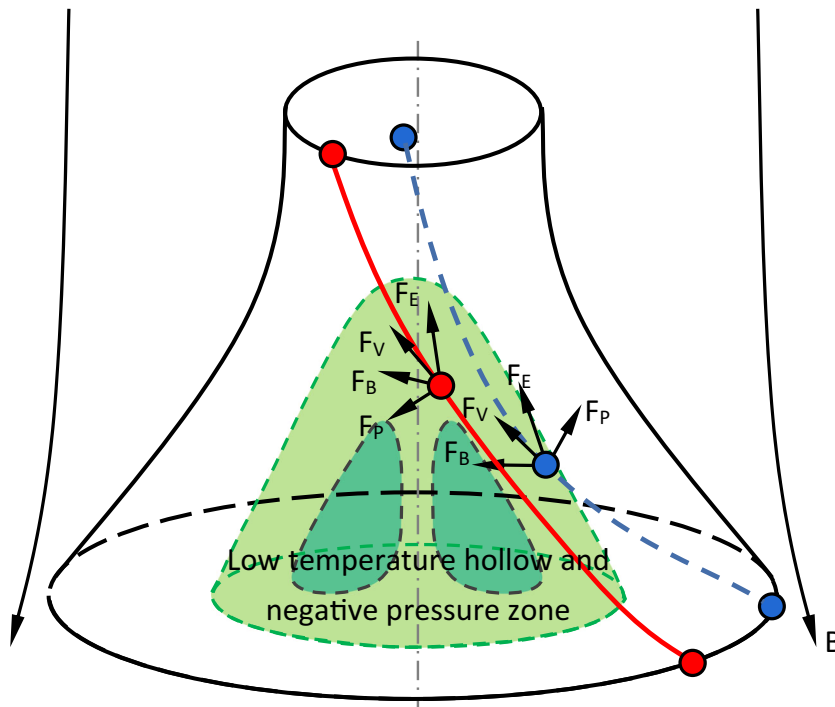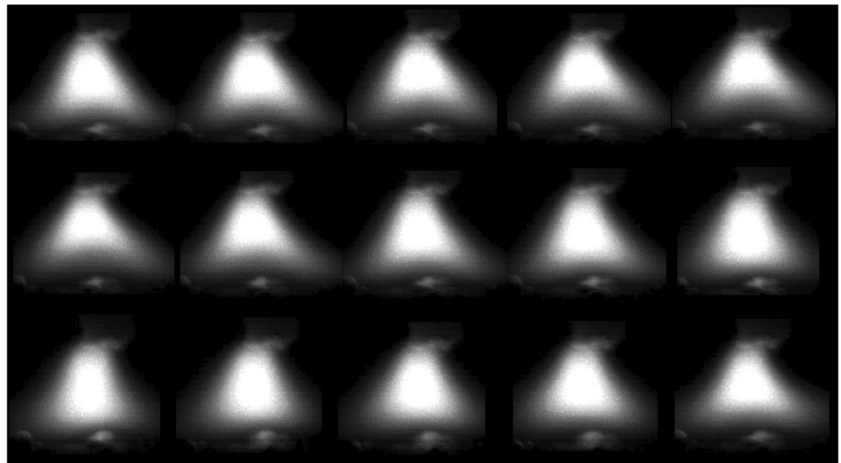Low temperature hollow and negative pressure zone

Fig. 12 Effects of low-frequency axial magnetic field direction on arc shape

disappear, the arc pressure increases, and the arc shrinks instantaneously. When the direction of the applied field does not change, the arc maintains a stable rotation state again, and the central negative pressure area increases again, and the arc expands [14]. When the magnetic field frequency is low, this phenomenon can be observed obviously. As shown in Fig. 12, the arc will continue to expand. When the magnetic field frequency is high, the arc still rotates at high speed, and the rotation direction changes rapidly with the increase of magnetic field frequency, and the charged particles always keep gathering under the tungsten electrode. Therefore, the arc shape is stable, the luminous region of the arc is lengthened and the central negative pressure area disappears, the arc pressure increases, and the arc shrinks significantly, as shown in Fig. 13. The induction heating effect of alternating magnetic field will help to improve the arc temperature, while the increase of arc plasma temperature increases the dynamic viscosity of the gas nearby, which hinders the outward movement of particles in the arc plasma. At the same time, both the annular Hall current generated by Hall effect and the induced current can promote the contraction of the arc [15]. In addition, the greater the magnetic induction intensity, the denser the magnetic lines, and the greater the magnetic frequency, the more uneven the distribution of magnetic lines inside and outside the arc, resulting in the magnetic pressure difference pointing to the inside of the arc plasma. All of these result in a significant contraction of the arc.

The forces exerted on the melt in the weld pool are shown in Fig. 14. There are six forces on the weld pool surface: the surface tension σ, the radial shear stress Frs, the circumferential shear stress Fcs, the electromagnetic force Fam produced by the external magnetic field, the electromagnetic force Fem produced by induced magnetic field, and the arc pressure Fpa. Under the influence of the applied DC or low-frequency axial magnetic field, the fluid in the weld pool flows outwards at the surface, downwards in the periphery of the molten pool, and upwards in the central region of the molten pool; as a result, the weld pool becomes wider and shallower [7]. When the high-frequency alternating axial magnetic field is applied, eddy current will be generated on the plane perpendicular to the magnetic lines inside the molten pool, and the additional eddy current force Fv will be generated by the interaction with the high-frequency alternating magnetic field. Due to the high density of magnetic lines in the upper part of the weld pool, the direction of resultant force Fv is shown in the Fig. 14. Therefore, in addition to the above six forces, the molten pool is also affected by buoyancy force Fb, gravity G, and eddy current force Fv. Compared with the traditional TIG welding, the movement of the melt in the weld pool is more complicated, and the stirring is more intense with the high-frequency alternating axial magnetic field, especially the electromagnetic force and eddy current force promote the melt flow downwards and towards the center of the molten pool. Meanwhile, because of the arc contraction and the increase of arc pressure, the weld penetration increases significantly, and the weld depth to width ratio increases finally, as shown in Fig. 7.

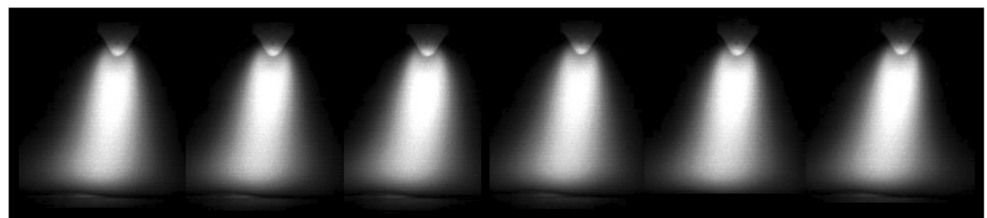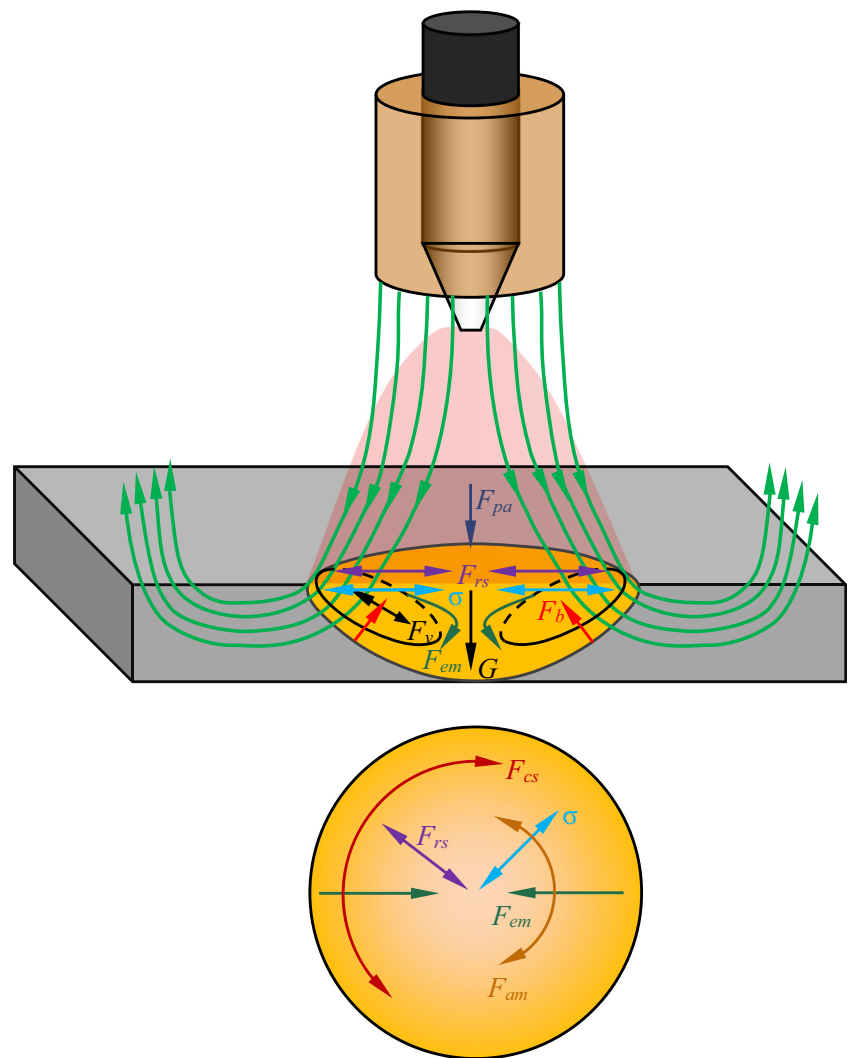**Fig. 13** Effects of low-frequency axial magnetic field direction on arc shape (1200 Hz)

Fig. 14 Schematic illustration of driving forces on the weld pool

4 Conclusions

Based on experimental and theoretical analysis, the influences of the external high-frequency alternating axial magnetic field on the properties of arc plasma, the flow behavior of the weld pool and the weld formation are investigated. The main conclusions are summarized as follows:

(1) Using the excitation coil installed on the TIG welding torch to generate an alternating HFAMF can significantly increase the welding penetration of TIG welding, thereby improving welding efficiency significantly, although additional magnetic heads may affect welding accessibility and increase production costs slightly. This technology will be widely used in the welding of non-ferrous metal medium and thick plates, the arc surfacing, and arc additive manufacturing.

(2) The external alternating HFAMF causes the arc to rotate, and as the frequency of the external magnetic field increases, the frequency of changing the direction of arc rotation increases.

(3) The low-frequency external axial magnetic field causes the arc to expand, the temperature and pressure of the arc center decrease, and the weld penetration depth decreases; but the high-frequency magnetic field can cause the arc to compress, the temperature and pressure of the arc center to increase, and the weld penetration depth to increase noticeably. That shows the significant effect of magnetic confinement of arc plasma and potential applications in industry.

(4) The effect of arc compression is most evident when the welding current is 70 A, the excitation current is 2 A, the magnetic field strength is 30 mT, the magnetic field frequency is 1500 Hz, and the weld penetration is maximum, about 43% higher than the arc with no applied field.

(5) The superposition of induced electromagnetic field caused by high-frequency magnetic field leads to uneven

distribution of magnetic field that generates magnetic pressure radially in the arc plasma. The radial magnetic pressure is the key factor for the magnetic compression of arc plasma when high frequency is applied.

References

1. Wu H, Yunlong C, Lu L, Jin B (2017) Review on magnetically controlled arc welding process. Int J Adv Manuf Technol 91(9–12): 4263–4273. https://doi.org/10.1007/s00170-017-0068-9

2. Yunlong C, Mingxu L, Lu L, Babkin AS, Lee B-Y (2015) Influence of longitudinal magnetic field on the CO_2 arc shape. Plasma Sci Technol 17(4):321–326. https://doi.org/10.1088/1009-0630/17/4/11

3. Kazufumi N, Kazuyuki M, Yoshinori H (2009) Magnetic control of arc plasma and its modelling. Weld World 53(7):181–187. https://doi.org/10.1007/BF03266730

4. Li Y, Wu CS, Wang L, Gao JQ (2016) Analysis of additional electromagnetic force for mitigating the humping bead in high-speed gas metal arc welding. J Mater Process Technol 229:207–215. https://doi.org/10.1016/j.jmatprotec.2015.09.014

5. Qingjie S, Wang J, Chunwei C, Qian L, Jicai F (2016) Optimization of magnetic arc oscillation system by using double magnetic pole to TIG narrow gap welding. Int J Adv Manuf Technol 86(1–4):761–767. https://doi.org/10.1007/s00170-015-8214-8

6. Wang X, Liang W, Suhong S (2013) The influence of rotating magnetic field on DCEN MAG industry welding based on properties of welding materials. Adv Mater Res 675:148–151. https://doi.org/10.4028/www.scientific.net/AMR.675.148

7. Xianqing Y, Jianjun G, Jianxun Z, Jiangtao S (2012) Numerical study of arc plasmas and weld pools for GTAW with applied axial magnetic fields. J Phys D Appl Phys 45(285203):1–13. https://doi.org/10.1088/0022-3727/45/28/285203

8. Tang C, Xiaoning Z, Bing B, Xu Z, Wang C, Weidong X (2015) Numerical study of DC argon arc with axial magnetic fields. Plasma Chem Plasma Process 35:61–74. https://doi.org/10.1007/s11090-014-9592-7

9. Zhengjun L, Yuhang L, Yunhai S (2018) Simulation and analysis of heat transfer and fluid flow characteristics of arc plasma in longitudinal magnetic field-tungsten inert gas hybrid welding. Int J Adv Manuf Technol 98:2015–2030. https://doi.org/10.1007/s00170-018-2320-3

10. Lincun L, Bing B, Zhipeng Z, Weidong X (2008) Axial magnetic-field effects on an argon arc between pin and plate electrodes at atmospheric pressure. IEEE Trans Plasma Sci 36(4):1078–1079. https://doi.org/10.1109/TPS.2008.920893

11. Xiaohong Z, Jingqing C, Kang Z, Ma P, Hui C (2019) Numerical investigation of coupled arc and electrode for GTAW with a longitudinal electromagnetic field. Int J Mod Phys B 33(1940033):1–9. https://doi.org/10.1142/S0217979219400332

12. Lei X, Ding F, Jiankang H (2018) Tungsten cathode-arc plasma-weld pool interaction in the magnetically rotated or deflected gas tungsten arc welding configuration. J Manuf Process 32:127–137. https://doi.org/10.1016/j.jmapro.2018.01.026

13. Luo J, Zongxiang Y, Xue K (2016) Anti-gravity gradient unique arc behavior in the longitudinal electric magnetic field hybrid tungsten inert gas arc welding. Int J Adv Manuf Technol 84(1–4):647–661. https://doi.org/10.1007/s00170-015-7728-4

14. Lei X, Ding F, Jiankang H (2018) Numerical simulation of unsteady arc in GTAW with alternate axial magnetic field. J Mech Eng 54(16):79–85. https://doi.org/10.3901/JME.2018.16.079

15. Lei X, Ding F, Jiankang H, Wang X (2018) Numerical simulation of TIG welding arc with extra high-frequency longitudinal magnetic field. Trans China Weld Inst 38(2):66–70